

## Excitons in bundles of single walled carbon nanotubes

M. Zamkov<sup>a,b,\*</sup>, A. Alnaser<sup>a</sup>, Z. Chang<sup>a</sup>, P. Richard<sup>a</sup>

<sup>a</sup> School of Chemical Sciences, University of Illinois at Urbana-Champaign, Box 71-6 CLSL, 600 South Mathews Avenue, Urbana, IL 61801, USA

<sup>b</sup> James R. Macdonald Laboratory, Department of Physics, Kansas State University, Manhattan, KS 66506-2604, USA

Received 14 November 2006; in final form 30 January 2007

Available online 9 February 2007

### Abstract

Time-resolved photoemission was used to differentiate between excitons and free carriers in non-fluorescing bundles of single walled carbon nanotubes (SWNT). Present findings show that direct interband excitations in semiconductive SWNTs lead to the formation of strongly bound excitons, indicating that proximity effects in SWNTs bundles do not destroy a one-dimensional character of optical excitations.

© 2007 Published by Elsevier B.V.

Systems exhibiting one-dimensional (1D) electron confinement have long fascinated scientists due to their unusual electrical and optical properties. The microscopic origin underlying this behavior is the significant enhancement in Coulomb interaction that only permits collective multi-particle excitations, leading to the formation of strongly correlated electron–hole (e–h) pairs, known as excitons [1]. Semiconductive SWNTs are one of the most interesting representations of such systems where the excitonic nature of optical excitations was manifested by the emission of fluorescence (FL) arising from the recombination of bound e–h pairs [2–5]. Until now, FL emission was observed only in nanotubes that were isolated from their environment by encapsulating in SDS micelles [6]. On the other hand, when their natural surroundings are not chemically suppressed, smooth-sided SWNTs readily aggregate into bundles, in which case no FL signal is detected [7]. This poses considerable experimental challenges for studying the dynamics of excitons in interacting SWNTs, raising a question if strongly bound e–h pairs even exist in nanotube bundles. According to several experimental reports, the intertube interaction in aggregated SWNTs unlocks

the carrier tunnelling mobility and, in principal, could wipe out the reduced dimensionality of e–h excitations [8,9]. In this case, some basic photoelectrical properties of bundled SWNTs such as the carrier photogeneration and the spatial separation of opposite charges would be substantially different from those of isolated nanotubes. Resolving these issues, for the most part, depends on our ability to probe the character of optical excitations in non-fluorescing bundles, favoring an experimental approach that does not rely on FL emission.

Here, we use the time-resolved electron emission spectroscopy to differentiate between excitons and free carriers in optical excited SWNT bundles. The selectivity of this approach is based on the strong suppression of non-resonant absorption in excitonic pairs, which distinguishes them from unbound carriers. Present data provides compelling evidence that most of e–h excitations in aggregated semiconductive (S) SWNTs form 1D excitons that remain bound for at least 0.5 ps. The delayed injection of free carriers into S nanotubes was also observed when the excitation pulse was resonant with the subband transitions in metallic (M) SWNTs, indicating a possibility of electron exchange between M and S species within a bundle.

Measurement of the emitted photoelectron energy distribution provides a versatile way of probing the dynamics of e–h pairs in optically inactive SWNT bundles. From the spectroscopic perspective, the recorded photoelectron

\* Corresponding author. Address: School of Chemical Sciences, University of Illinois at Urbana-Champaign, Box 71-6 CLSL, 600 South Mathews Avenue, Urbana, IL 61801, USA.

E-mail address: [zamkov@uiuc.edu](mailto:zamkov@uiuc.edu) (M. Zamkov).

signal is proportional to the amount of free e–h pairs generated by the laser pump-pulse [10], and, therefore, can be used to obtain the energy-dependent carrier intensity distribution. This approach, however, cannot be directly applied for interpreting the electron emission from excitons, as the mechanism of carrier photoionization in this case is fundamentally different. The main distinction is the requirement for a photon-assisted dissociation of a correlated pair, which is subject to energy and momentum constraints. Previously, the break-up of excitonic bonds has been investigated in relation with the temperature induced photogeneration of carriers [11] and is well described by the theory of Onsager [12]. The probability for the dissociation of an exciton reaches its maximum when the energy of the probe-photon,  $E_P$ , matches the exciton binding energy,  $E_B$ , and falls off quickly as  $E_P$  increases [13]. In present experiments,  $E_B \approx 0.15$  eV [14]  $\ll E_P$ , which, according to the low order single particle–hole pair approximation [13] leads to the significant reduction of the dissociation probability in comparison to resonant conditions. As a result, the photoemission from excitons, is expected to be strongly suppressed. This behavior has been demonstrated in excited state photoemission experiments on  $C_{60}$  molecules [15], where the emission from bound e–h pairs was found to be considerably weaker than that of free carriers. Accordingly, in this work we rely on the blockage of UV-photoemission from excitons for selective measurements of free carrier distribution in nanotube bundles. This approach, combined with the proportional to the total number of excited e–h pairs absorption spectroscopy is used to estimate the fraction of excitons among all optical excitations.

The nanotubes investigated in this work were produced by electric arc discharge technique and then used to fabricate 1-mm-thick bucky paper. The purity of the samples was analyzed through solution-phase near-IR spectroscopy, indicating a presence of approximately 10% of carbonaceous impurities [16,17]. The aggregation of most nanotubes into bundles was verified by scanning electron microscopy of solid samples [16]. In general, electronic properties of bundled SWNTs can be displayed through the schematic density of states (DOS) for both metallic (M) and semiconductive (S) nanotubes, which is shown in Fig. 1. The S SWNTs are identified by the first two well-defined state density gaps, denoted as A and B, while the larger opening in DOS (C) corresponds to M SWNTs [16]. In the present work, the associated subband transitions have been categorized by means of optical absorption spectroscopy, revealing the characteristic structure, shown in Fig. 2 by a solid line. Owing to the high-purity of SWNT samples [17], the resonant absorption peaks A–C can be clearly identified above the background. From the observed transition energies we deduce the average nanotube diameter of 1.32 nm, as well as the standard deviation for the diameter distribution (0.15 nm).

In the time-resolved photoemission (TRPE) study, the selective excitation of e–h pairs in both S and M nanotubes

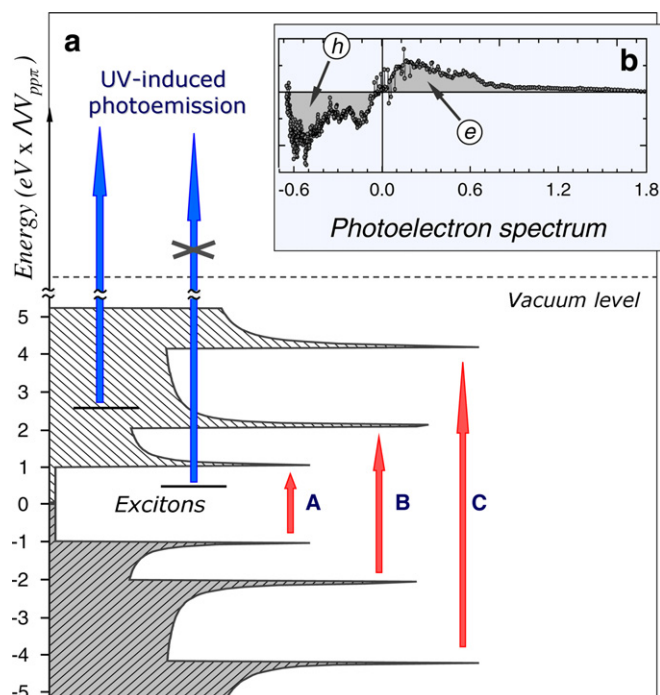


Fig. 1. Schematic density of electronic states for a nanotube bundle that includes features of both S and M SWNTs. (a) Two-photon excitation scheme utilizing the tunable pump and photoemission probe. The energy scale is given in units of  $\Lambda/V_{pp}$ , where  $\Lambda$  is the dimensionless ratio of the nanotube diameter to the carbon–carbon bond distance and  $V_{pp} \approx 2.5$  eV is a hopping integral. (b) A typical two-photon photoelectron spectrum, reflecting the e–h distribution near  $E_F$ , approximately 50 fs after the excitation pulse.

was done by tuning the 50 fs pump-pulses from 600 to 1900 nm, which covered the full range of resonant transitions (A–C). The resulting excited carrier distribution was then probed with fixed-energy UV photons that exceeded the sample work function by approximately 0.5 eV. Following the photoionization, electrons drifted into the magnetically and electrically shielded 30-cm-long spectrometer tube and were detected with a backgammon position sensitive detector. The accumulated electron time-of-flight was then converted to the excitation energy ( $E-E_F$ ) with an average uncertainty of 20 meV.

Fig. 1b shows a characteristic, background-subtracted photoelectron spectrum. The positive side ( $E > 0$ ) reflects the energy distribution of electrons in the conduction band, whereas the emission associated with the negative values of  $E$  represents the distribution of holes left behind in the valence band by the excitation pulse [18]. Notably, the energy of the highest occupied electronic state (see Fig. 1b) coincides with the photon energy ( $\approx 1.6$  eV) used for the excitation step in this case, indicating a single-photon excitation regime.

The TRPE signal was integrated over the electron energy for a fixed excitation wavelength and compared to the absorption spectrum in Fig. 2. One apparent trend, evident from the comparison, is the absence of almost any photoemission from S nanotubes, which is indicated by a

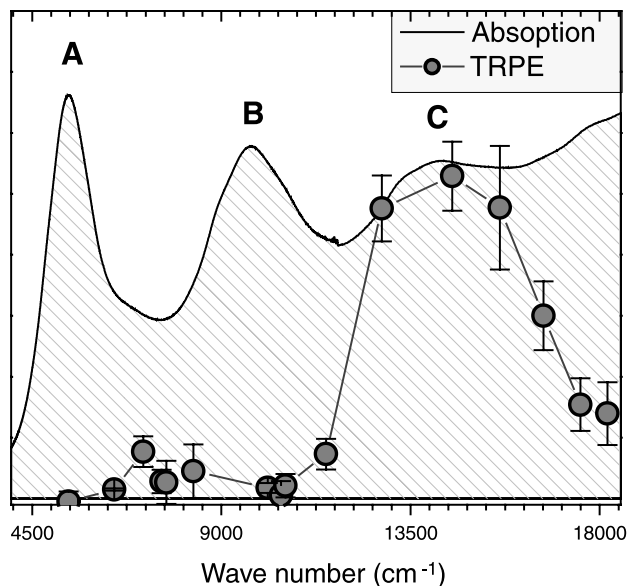


Fig. 2. Comparison of the optical absorption and TRPE measurements. The absorption spectrum shows the first (A) and the second (B) subband transitions in S SWNTs and the first subband transition (C) in M SWNTs. The time-resolved photoemission signal, collected 50 fs after the pump pulse, is plotted versus the wave number of the excitation photon. The maximum of the photoemission is detected when the excitation wavelength is resonant with C transitions in M nanotubes. Notably, almost no photoemission is detected from semiconductive nanotubes. The experimental error bars denote the absolute uncertainty of the TRPE measurements.

vanishing signal near absorption peaks A and B. This is particularly eminent in contrast to the strong photoelectron peak around C transitions in M nanotubes that are primarily populated by ‘visible’ to the photoemission probe free carriers. We note that the total amount of excited pairs in S nanotubes is comparable to that of M SWNTs, as can be evidenced by the nearly equal absorbance for the three resonant peaks in Fig. 2, and the much weaker photoemission from the A and B subbands is simply caused by the lack of free e–h pairs in S species. This detail is also seen in the differential TRPE spectra, recorded for the three cases of resonant excitation near absorption maxima (A–C) (see Fig. 3). In contrast to the well defined bipolar-shaped e–h distribution, observed when the pump wavelength is resonant to the C transition in M SWNTs (Fig. 3a), the TRPE signal resulting from the excitation of A and B band gaps in S nanotubes (Fig. 3b and c) cannot be distinguished. In fact, no detectable photoemission was observed even after the pump intensity in the spectral range of A and B transitions was increased by almost an order of magnitude with respect to that of C peak! Such a strong suppression of photoelectron response from bundled S SWNTs indicates that excitonic pairs account for the most of e–h excitations in these tubes.

While the formation of excitons in bundles is likely governed by the same excitation mechanism as those in individual S nanotubes, their recombination dynamics is uniquely different, as exemplified by the absence of radiative

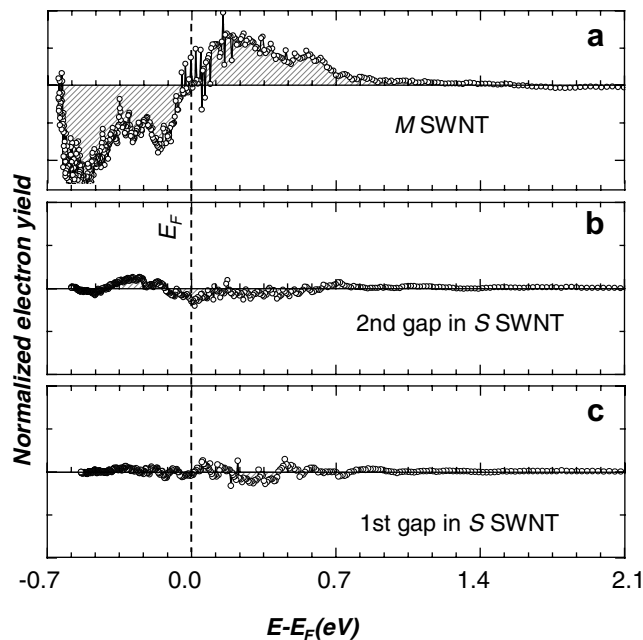


Fig. 3. Energy dependence of the electron distribution measured 50 fs after the excitation pulse with photon energies of 0.68 eV (a), 1.25 eV (b), and 1.83 eV (c). (a) Excitation photon is resonant with the first subband transition in M nanotubes. (b, c) Excitation photon is resonant with the second and the first subband transitions in S nanotubes, respectively.

ative decay in aggregated SWNTs. To gain a better understanding of the carrier mobility in bundles, we performed the time-dependent study of the excited state population. First, we look into the delayed photoelectron signal arising from A and B subband excitations in S nanotubes. Similar to the case when the pump and probe pulses nearly overlap in time, shown in Fig. 2, no detectable emission was observed for the investigated delay range of 50–500 fs. The absence of free carriers in S subbands indicates that the dominant portion of e–h pairs remain bound. This short-term stability of excitons, however, does not rule out their subsequent non-radiative annihilation, as the investigated time scale constitutes only a small fraction of the excitonic radiative lifetime. Nevertheless, the half-picosecond stability indicates that excitons are unaffected by thermal perturbations and, thus, bound by energies in the excess of the room-temperature  $kT$ . This is an important result as it demonstrates a large degree of carrier confinement in bundled S SWNTs, indicating a low-dimensional character of excitations.

The temporal evolution of excited population in M nanotubes is shown in Fig. 4. Previous studies [19,20] have demonstrated that the energy distribution of free carriers in this case, reflects the net change in the Fermi–Dirac thermal distribution,  $\Delta f = f(T_e) - f(T_{ion})$ , where  $T_e$  is the temperature of the electronic system heated by a laser pump-pulse. Typically, a very good fit of experimental data could be obtained with the  $\Delta f(T_e)$  functional form as was previously demonstrated for the case of non-resonantly excited SWNT bundles [19] as well as MWNTs [20]. In

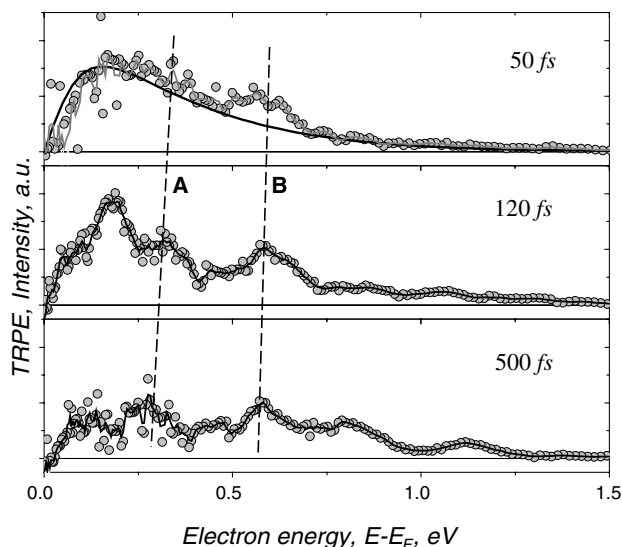


Fig. 4. Time dependence of the electron emission from resonantly excited metallic nanotubes. Peaks A and B are found near the expected positions of the first two subband transitions in S SWNTs ( $E_A \approx 0.27$  and  $E_B \approx 0.54$  eV [21]).

present measurements the energy dependence of the electron yield also exhibits the known Fermi–Dirac trend, shown by the solid line in the upper panel of Fig. 4. In addition to the thermal distribution of free carriers, the spectra also reveals the two peaks (marked as A and B), located approximately 0.3 and 0.55 eV above the Fermi level, that become slightly more eminent at longer delays. The origin of this emission cannot be attributed to excitations in M SWNTs as the peaks' positions are far below the first van Hove singularity (C) and significantly above the thermal distribution of electrons at  $E_F$ . Instead, the energies of the peaks (denoted by slanted lines in Fig. 4) fall within the expected positions of resonant transitions in the investigated S nanotubes,  $E_A \approx 0.27$  and  $E_B \approx 0.54$  eV [21], and were accordingly identified as originating from A and B subbands. The maximum of the electronic population in these bands reflects an instantaneous 'electronic temperature', associated with non-equilibrium electron distribution immediately after excitation [20]. At longer pump-probe delays, the electronic system cools down through electron–phonon interaction and relaxes to the band edge [19]. This results in an energy shift in the maximum of electronic distribution, which is denoted in Fig. 4 by slanted lines.

Interestingly, the presence of semiconductive peaks A and B in electron spectra is detected only when the excitation energies are near the interband transitions in M nanotubes. This suggests a possible correlation between the population of conduction states in M nanotubes and the injection of free carriers into S bands. It could be argued that the excitation of S peaks, A and B, is due to the non-resonant pumping of S subbands and not due to the excitation of M transitions. In this case, however, the same

S states should be populated during the non-resonant excitation with photon energies that are immediately below the interband transition energy in M SWNTs. This, however, does not occur, since the energy-integrated photoemission for this excitation window of  $9000\text{--}10000\text{ cm}^{-1}$ , shown in Fig. 2B is virtually zero. We thus speculate that the presence of free carriers in S nanotubes could be due to electron tunnelling from M species. This result is consistent with earlier findings suggesting the possibility of tunnel coupling between S and M bundled nanotubes [8,9].

In summary, by monitoring the electron emission from non-fluorescing nanotube bundles, we have investigated the nature of optical excitations in aggregated SWNTs. We have shown that direct interband excitations in S SWNTs lead to the formation of strongly bound excitons, indicating that proximity effects in SWNTs bundles do not destroy the 1D character of optical excitations. We have also observed that a detectable amount of unbound carriers is injected in excited states of S SWNTs when the excitation energy is near interband transitions in M nanotubes.

#### Acknowledgements

Authors would like to acknowledge Dr. Mikhail Itkis at University of California, Riverside, for help related to absorption spectra and purity evaluation. This work was supported by Chemical Sciences, Geo-sciences and Biosciences Division, Office of Basic Energy Sciences, Office of Science, US Department of Energy.

#### References

- [1] M. Pope, C.E. Swenberg, *Electronic Processes in Organic Crystals and Polymers*, second edn., Oxford University Press, New York, 1999.
- [2] C.L. Kane, E.J. Mele, *Phys. Rev. Lett.* 90 (2003) 207401.
- [3] S.M. Bachilo et al., *Science* 298 (2002) 2361.
- [4] H. Htoon, M.J. O'Connell, P.J. Cox, S.K. Doorn, V.I. Klimov, *Phys. Rev. Lett.* 93 (2004) 027401.
- [5] F. Wang, G. Dukovic, L.E. Brus, T.F. Heinz, *Science* 308 (2005) 838.
- [6] M.J. O'Connell et al., *Science* 297 (2002) 593.
- [7] A. Thess et al., *Science* 273 (1996) 483.
- [8] S. Reich, M. Dworzak, A. Hoffmann, C. Thomsen, M.S. Strano, *Phys. Rev. B* 71 (2005) 033402.
- [9] J.S. Lauret, C. Voisin, G. Cassaboiss, C. Delalande, P. Roussignol, O. Jost, L. Capes, *Phys. Rev. Lett.* 90 (2003) 057404.
- [10] J. Bokor, *Science* 246 (1989) 1130.
- [11] R. Kersting et al., *Phys. Rev. Lett.* 73 (1994) 1440.
- [12] D.M. Pai, R.C. Enck, *Phys. Rev. B* 11 (1975) 5163.
- [13] M.A. Nazar, J.C. Polanyi, W.J. Skrlac, *Chem. Phys. Lett.* 29 (1974) 473.
- [14] T.G. Pedersen, *Phys. Rev. B* 67 (2003) 073401.
- [15] J.P. Long, S.J. Chase, M.N. Kabler, *Chem. Phys. Lett.* 347 (2001) 29.
- [16] M. Itkis et al., *Nano Lett.* 3 (2003) 309.
- [17] NanoLab, Inc., 55 Chapel Street Newton, MA 02458.
- [18] M. Zamkov, N. Woody, B. Shan, Z. Chang, P. Richard, *Phys. Rev. Lett.* 94 (2005) 056803.
- [19] T. Hertel, G. Moose, *Phys. Rev. Lett.* 84 (2000) 5002.
- [20] M. Zamkov, N. Woody, B. Shan, Z. Chang, P. Richard, *Appl. Phys. Lett.* 89 (2006) 093111.
- [21] J.W. Mintmire, C.T. White, *Phys. Rev. Lett.* 81 (1998) 2506.